INSTITUTE OF PHYSICS PUBLISHING JOURNAL OF MICROMECHANICS AND MICROENGINEERING

J. Micromech. Microeng. **16** (2006) 480–486 doi:10.1088/0960-1317/16/3/002

Fuse-tethers in MEMS

Yu-Shan (Susan) Chiu, Kwan-Shi (Jason) Chang, Robert W Johnstone and M Parameswaran

Institute for Micromachine and Microfabrication Research, School of Engineering Science, Simon Fraser University, 8888 University Dr. Burnaby, BC, V5A 1S6, Canada

E-mail: param@cs.sfu.ca

Received 24 October 2005, in final form 22 December 2005
Published 25 January 2006
Online at stacks.iop.org/JMM/16/480

Abstract

During the fabrication of freestanding micromechanical structures, the structures must often be attached to the substrate to prevent movement, particularly during the release process. The attachments are then removed, freeing the structures from the substrate when they are to be used. Tethers are long thin beams that mechanically anchor freestanding structures to the substrate during fabrication, but are easily broken afterwards. This paper focused on fuse-tether designs and the associated technique used to break the tethers, Joule heating. The breaking characteristics of two fuse-tether designs were investigated using different current pulses. For each design, the current pulse that produced the most desirable electrical and mechanical break was chosen for reliability testing. The reliability tests resulted in a 100% success rate. However, molten silicon splattered undesirably in 20% of the cases. In addition to empirical testing, ANSYS® was used to simulate the Joule heating process. The ANSYS® model produced results that closely matched the break characteristics observed in the empirical tests. This research demonstrated that a fuse-tether can be severed reliably with the Joule heating technique, and the fuse-breaking characteristics can be predicted by modeling.

(Some figures in this article are in colour only in the electronic version)

1. Introduction

Microelectromechanical systems (MEMS) are systems that integrate electrical and mechanical components on a common substrate. The micromechanical structures in surface-micromachined MEMS are often designed to be freestanding during operation [1, 2]. However, these freestanding structures can pose a reliability problem during fabrication, because they can shift and damage surrounding devices as well as themselves during the release step [3–7]. To prevent damage during and after fabrication, tethers are used to attach the freestanding structures to the substrate. When the structures are ready to be used, the tethers are broken, which release the freestanding structures from the substrate.

While necessary, conventional tethers suffer a number of disadvantages. Because they are designed to be broken using the micro-positioners of a microelectronics probing station, they require enough chip area for the probe tips to safely land on the surface without damaging nearby structures. Additionally, breaking the tethers is a serial process, and not easily scaled to manufacturing. We thus began looking for a replacement.

In this paper, a technique for breaking tethers that uses Joule heating is investigated. With this technique, the mechanical connection is broken in a manner analogous to electrical fuses. For this reason, the class of tether designs investigated is called fuse-tethers.

To break a tether, a large current is passed through the tether. The associated Joule heating causes a large increase in temperature, which in turn causes the tether material to either melt or vaporize. This melting not only breaks the electrical connection, but also breaks the mechanical connection. Joule heating is an attractive approach to breaking the tethers, because electrical connections to on-chip components are relatively easy to make and automate in comparison with other techniques, such as physical breaking or laser ablation.

Furthermore, because fuse-tethers do not require physical access, they require significantly less immediate chip area. Thus, the tethers allow higher packing of mechanical components. However, when bonding pads and wiring

are included, the devices do occupy more chip area than conventional tethers. However, we hope in the future to extend the work presented here to provide a means of breaking multiple tethers using the same electrical connections. With the area of the bonding pads amortized over multiple tethers, this approach will use less chip area than conventional tethers.

Microfabricated polysilicon fuses have been investigated before [8–11]. However, these devices were purely electrical fuses, with two electrical terminals. The fuse-tethers discussed in this paper have three terminals, two electrical and one mechanical. In the operation of fuse-tethers, it is critical that all three terminals be severed simultaneously.

A theory on fuse-tether Joule heating is discussed in this paper. ANSYS® models were also developed to simulate the fuse-tether breaking process. Both the closed-form and numerical results were compared to experimental data.

2. Theory

2.1. Joule heating

Joule heating is a phenomenon that occurs when an electrical current flows through a resistive material. The electrical power dissipated is converted to heat, which causes the material's temperature to rise [12]. The resistance of a material is defined by the following equation:

$$\mathrm{d}R = r\frac{\mathrm{d}L}{A}. \tag{1}$$

In equation (1), L is the length, r is the resistivity and A is the cross-sectional area.

If one imagines partitioning the fuse-tether into infinitesimal sections, where each section has the same length and resistivity, the resistance of each section depends only on the cross-sectional area. Thus, the narrower regions of a fuse-tether have higher resistances. High resistance leads to greater Joule heating, causing the narrow parts of a fuse-tether to heat up faster. The material in the narrow regions thus melts sooner, and this breaks the tether. By properly designing the geometry, one can selectively choose which areas of the fuse-tether will melt first under the applied current.

The process does, however, require a degree of control. Providing too little energy to the fuse-tether does no damage, or breaks the electrical connection without breaking the mechanical connection. Conversely, providing too much energy leads to collateral damage. One would thus like to determine the ideal amount of energy required to break a fuse-tether.

2.2. Melting energy

The total amount of energy required to break a fuse-tether involves providing sufficient heat to raise the tether's temperature from room temperature to the material's melting point, and to transform the material from solid to liquid phase. The latter being described by the latent heat of fusion. The total melting energy is summarized by equation (2), where C_P is the specific heat capacity of the tether material (for example, polysilicon), ΔT is the change in temperature to the melting point, l_F is the latent heat of fusion of polysilicon and m is the mass of the region to be melted:

$$E_\mathrm{melt} = C_\mathrm{P} m \Delta T + l_\mathrm{F} m. \tag{2}$$

In equation (2), the heat lost through thermal flow to the substrate was ignored, because the tethers are suspended above the substrate and in poor thermal contact. The Fourier number, described in section 2.4, will also be used to minimize heat dissipation. The heat lost through air is also neglected here, because the thermal conductivity of air is relatively small compared to the fuse-tether material, polysilicon [13].

2.3. Electric energy

The electrical energy for Joule heating was delivered into the tether using a current source. When using a current source, the series parasitic resistances do not affect the calculations. The amount of energy, E_elec, provided by the current source is given by equation (3), where P is the power, t is the time, I is the current amplitude and R is the resistance:

$$E_\mathrm{elec} = Pt = I^2 Rt. \tag{3}$$

By equating equation (2) to equation (3), one can calculate the necessary current to break the fuse-tether once the time, t, has been determined. To determine the time, the Fourier number must be investigated.

2.4. Fourier number

As mentioned in a previous section, the Fourier number is used to minimize the heat lost through conduction during the Joule heating process. The Fourier number, F_0, is a dimensionless number that is a measure of heat conducted through a body relative to the heat stored [14]. When sufficiently small ($F_0 \ll 1$), the dominant destination of Joule heating will be to increase the device's temperature, and little thermal energy will have time to dissipate.

For fuse-tethers, there are two advantages in choosing $F_0 \ll 1$. First, the ability to neglect heat conduction greatly simplifies the analysis. Second, and most importantly, it ensures that the heating is localized.

The Fourier number is given by equation (4), where k_T is the thermal conductivity, C_P is the specific heat capacity at constant pressure, ρ is the density and L_c is the characteristic length:

$$F_0 = \frac{k_\mathrm{T} t}{C_\mathrm{P} \rho L_\mathrm{c}^2}. \tag{4}$$

To break the fuse-tethers, we start with a Fourier number of 0.1. Then, using equation (4), the time-scale for melting the fuse-tethers can be calculated. For the devices reviewed in this paper, the times, which will be calculated later, are on the order of a microsecond. With this time in hand, the current pulse duration is known, and the necessary current can then be fully determined, using equations (2) and (3).

3. Fuse-tether design

The two fuse-tethers to be presented in this paper are designed and fabricated using a surface-micromachining process called the polysilicon multi-user MEMS processes (PolyMUMPs™) [15] provided by MEMSCAP. We named the first tether design the butterfly design, and the second design the 'T'-design.

The dimensions and photomicrograph of the butterfly tether are shown in figures 1(*a*) and (*b*), respectively. Although

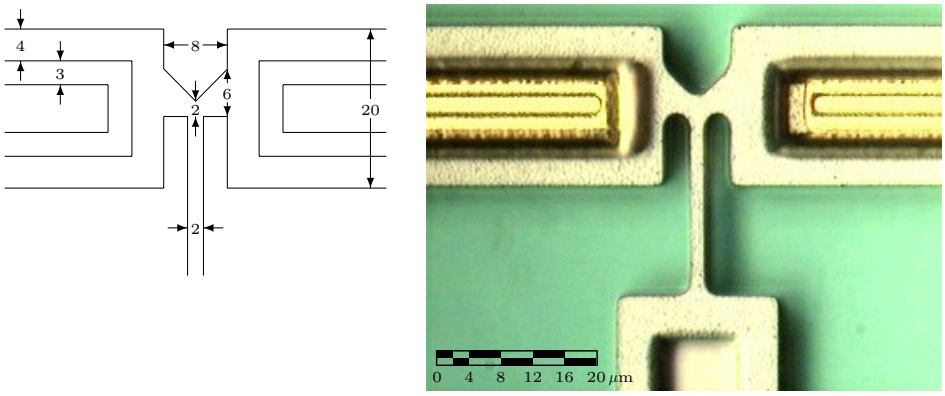

(*a*) (*b*)

Figure 1. Dimensions of layout for butterfly design and photomicrograph of the fabricated tether. (*a*) Dimensions (μm) and (*b*) photomicrograph.

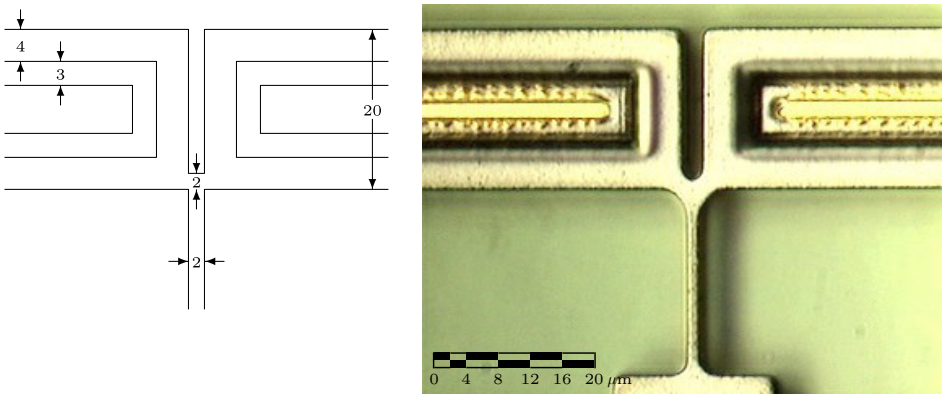

(*a*) (*b*)

Figure 2. Dimensions of layout for 'T'-design and photomicrograph of the fabricated tether. (*a*) Dimensions (μm) and (*b*) photomicrograph.

it is not apparent in the figures, the tether is suspended 2 μm above the substrate.

For the 'T'-design tether, its dimensions and photomicrograph are shown in figures 2(*a*) and (*b*), respectively. Again, the tether is suspended 2 μm above the substrate.

The photomicrographs of the butterfly and 'T'-design fuse-tethers do not exactly resemble the layouts because the corners are rounded during the reactive ion etching (RIE) used to pattern the devices.

Both types of fuse-tethers contain two electrical connections, which leave the fuse to the left and right in the figures, and one mechanical connection, which descend from the tether. All three connections meet at a single point that is designed to have maximum current density. The first design, the butterfly design, achieves this by concentrating the current at the point where the mechanical connection is made to the electric path. The second design, the 'T'-design, refined this concept to emphasize the concentration of current at the three-way junction. However, it was felt that the 'T'-design, because of the minimum feature size at the junction, would not be as manufacturable as the butterfly design. Therefore, both designs were manufactured. The butterfly design is more reliable, but for a reason other than manufacturability, which will be discussed later.

4. Experiment

Both designs were tested by applying square current pulses with varying currents and durations. The circuit used to deliver the current pulses was custom built [13], and is shown in figure 3. The circuit was designed to provide square current pulses with currents up to 400 mA for resistive loads up to 120 Ω. The circuit was tested against several resistors to confirm its range of operation, and to calibrate its output. During the testing, it was also found that the shortest pulse that the circuit can reliably generate is approximately 3.2 μs.

The circuit is composed of three stages. The first stage is a trigger circuit, the second stage is a monostable multivibrator and the third stage is a transconductance amplifier. The circuit contains two variable resistors: R_{D1} and R_E. The resistance of R_{D1} is used to control the duration of the pulse, while R_E is used to control the current of the pulse.

During testing of the fuse-tethers, the voltage across the device-under-test, i.e. the fuse-tether, was monitored using an oscilloscope. This not only provided confirmation that the correct current load was being applied, as the resistance of each tether was measured beforehand, but the waveform also indicated when the electrical connections broke.

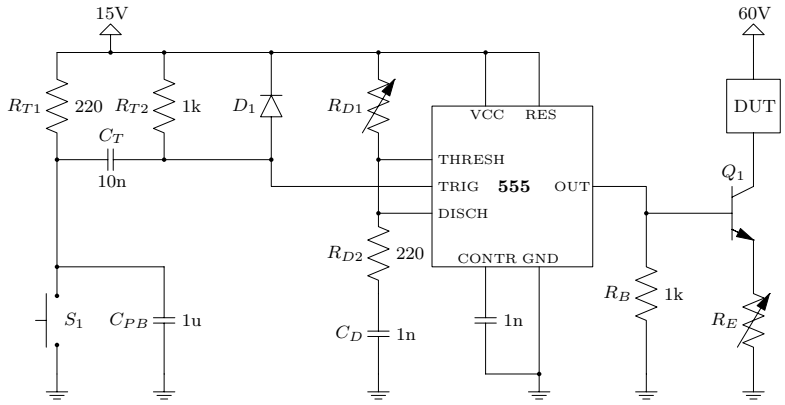

Figure 3. Schematic for circuit used to generate current pulses. Pulses are initiated by pressing switch S_1, and the current pulses pass through the device-under-test (DUT). Resistors R_{D1} and R_E are used to adjust the duration and magnitude of the current pulses, respectively.

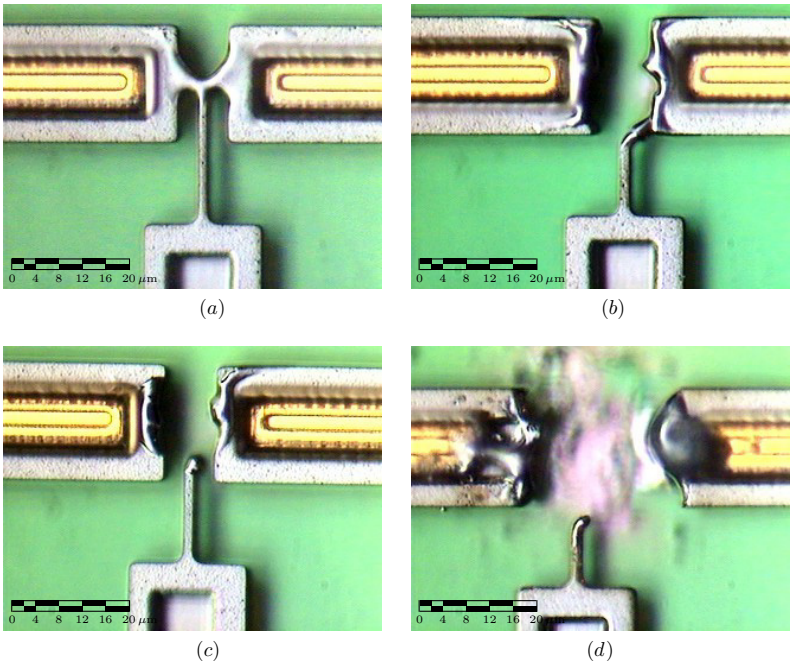

Figure 4. Photomicrographs of butterfly tethers after increasing currents. (*a*) Smoothing at the center of the butterfly tether indicates melting. (*b*) At higher currents, more melting occurs, but there is still insufficient energy to produce a clean physical break in the butterfly tether. (*c*) An ideal cut. (*d*) Splattering in the tether occurs when too much energy is supplied.

4.1. Butterfly design

A range of current amplitudes from 60 mA to 360 mA with different pulse widths was applied to the butterfly design. The range of behaviors observed over this current range is shown in figure 4. The results indicate that control of the energy delivered is important to successful operation.

When the supplied energy is only sufficient to melt the center of the tether and not enough to produce a clean physical break, the characteristics shown in figures 4(*a*) and (*b*) were observed.

On the other hand, if too much energy was supplied into the tether, excessive splattering of the molten polysilicon occurred, as shown in figure 4(*d*).

The current pulse producing the best reliability and consistency for the butterfly tether has a current of 288 mA and an average break time of 7 μs. The photomicrograph of an ideal butterfly tether cut is shown in figure 4(*c*).

It is important to note that the gold layer, present on the conducting lines adjoining the fuse, is not visibly affected when the melting process is properly controlled (figure 4(*c*)). Even in the case of excessive heat (figure 4(*d*)), the gold is still unaffected outside the region of polysilicon splatter. This indicates that at these points, the temperature is less than the melting point of gold, 1064 °C [16]. This should be compared to the temperature needed to melt the silicon, 1410 °C [16]. Therefore, even at this short distance from the fuse, the peak temperature has been considerably reduced. The localization of the temperature increase is a consequence of using the small Fourier number.

Using the current pulses of 288 mA and 7 μs, and with a sample size of 20, 100% butterfly cut rate was achieved,

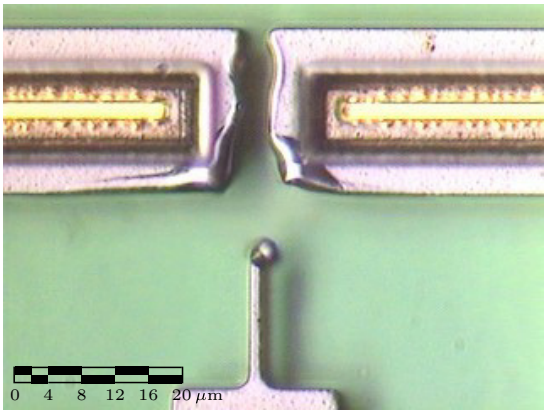

Figure 5. Photomicrographs of a 'T'-design tether after an ideal cut.

with 15% of the cuts resulting in some form of undesirable splattering. The photomicrograph illustrating the undesirable splattering in the butterfly design is shown in figure 4(*d*). The existence of polysilicon splatter indicates excessive heating.

The splatter could be the result of process variations across the die. Unfortunately, since the tethers were fabricated using the minimum allowable geometry, they exhibit the greatest relative variation. Smaller tethers have greater Joule heating, and thus may exhibit splatter even for current pulses properly designed for the nominal geometry. However, it is better to ensure that all of the tethers break, so we err on the side of excessive heating, rather than insufficient heating.

4.2. 'T'-design

For the 'T'-design tether, a range of current amplitudes from 208 mA to 300 mA was applied. Photomicrographs of the tethers afterwards show a similar range of behaviors as shown in figure 4. Complete cutting without splatter requires applying the current level of current.

For 'T'-design tethers, the current pulse producing the most reliable and consistent results has a magnitude of 264 mA and an average break time of 12 μs (figure 5). For a sample size of 20, this current pulse produced 100% cut rate, with 20% of the cuts resulting in some forms of undesirable splattering.

When the 'T'-design is overheated, pieces of melted polysilicon are prone to splattering beyond the immediate area of the tether, unlike the butterfly design. Even when the butterfly design has excessive splattering, the splatter is typically contained within the immediate area of the tether. The better containment occurs because the butterfly tether is located centrally between the contact arms. The contact arms act like barriers and contain any splattering.

5. Experiment versus theory

To determine the Fourier number, several material parameters and two design parameters are required. For the material parameters, the values $k_T = 34.613$ W m^{-1} K, $C_p = 871$ J kg^{-1} K and $\rho = 2330$ kg m^{-3} were used [13]. The two design parameters are the characteristic length, L_c, and the time, t.

Table 1. Experimental Fourier numbers.

Tether	Ideal F_0	Experimental F_0
Butterfly design	0.1	0.987
'T'-design	0.1	3.198

Table 2. Experimental melting energy.

Tether	Ideal E_{melt}	Experimental E_{melt}
Butterfly design	2.465×10^{-6} J	2.903×10^{-5} J
'T'-design	1.737×10^{-6} J	6.524×10^{-5} J

The characteristic length is taken to be the length of the shortest path through polysilicon from the center of the fuse-tethers to the substrate, which was taken as thermal ground. This works out to be $L_c = 11$ μm and $L_c = 8$ μm for the butterfly and 'T'-tethers, respectively [13].

The time was set to the pulse duration from the best cutting conditions, as empirically determined (section 4). Thus, the values of $t = 7$ μs and $t = 12$ μs were used for the butterfly and 'T'-tethers, respectively.

The experimental Fourier numbers are greater than 0.1 (table 1), which indicates that heat loss is greater than what was expected. Thus, one would expect that the amount of energy injected into the tether to be greater than the amount predicted by equation (2). Using the experimental current and time values, this was confirmed as shown in table 2.

6. ANSYS

6.1. Modeling

ANSYS® is a finite element analysis (FEA) tool that is capable of solving structural and thermal dynamics problems. We used this tool to simulate the fuse-tether designs.

First, the geometry of the fuse-tethers was built by importing an ANSYS® Neutral Format (ANF) script file created according to the original layout. The layout was exported as a CalTech Interchange Format (CIF) file. The CIF file was then converted to an ANF file using the layout2model software [17]. In addition to the fuse-tether itself, air volume was added to surround the tether to closely model the experimental condition.

After creating the physical model, SOLID69 was chosen as the element type to map the models. In this paper, the thermal responses of tethers after applying a constant current were studied. SOLID69 is the element type that can be used to model structural, electrical and thermal problems. However, only the electrical and thermal degrees of freedom were used.

Most of the material properties used in these simulations were taken from a paper on modeling electro-thermal effects in polysilicon [18]. Because that paper did not consider the properties of molten silicon, electrical and thermal conductivity data for molten silicon were used from alternate sources [19, 20].

Boundary conditions were applied to three regions of the model. The substrate was assumed to behave as a thermal ground. Therefore, the entire bottom of the model was set to room temperature. Further, the fuse crosses the outside edge of the model at two faces, which were used as the

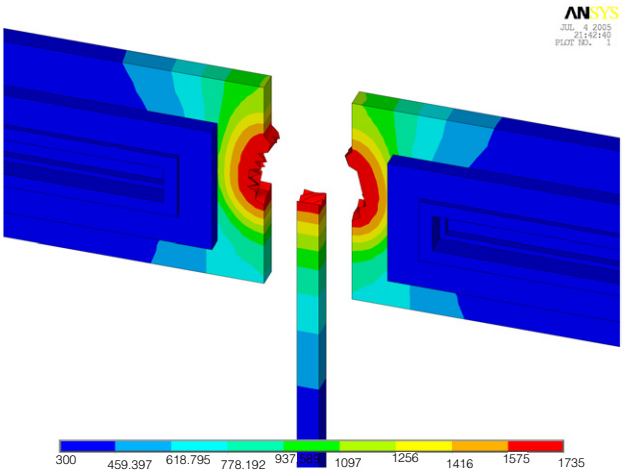

Figure 6. Finite element simulation of butterfly fuse-tether with current $I = 288$ mA and pulse width $t = 7$ μs. Regions hotter than the melting point were removed from the illustration for comparison with photomicrographs.

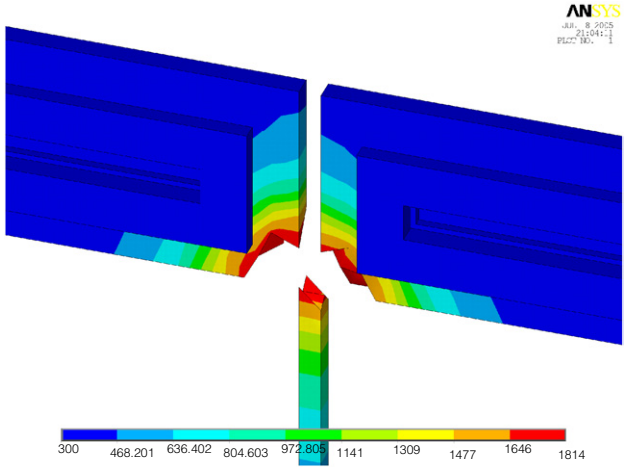

Figure 7. Finite element simulation of 'T' fuse-tether with current $I = 264$ mA and pulse width $t = 12$ μs. Regions hotter than the melting point were removed from the illustration for comparison with photomicrographs.

electrical terminals for the device. One face was set to ground, while a constant current was distributed evenly over the other to simulate the constant current source, as described in section 4.

6.2. Simulation result for butterfly design

By applying the same current to the ANSYS model as was used in the experiment, the simulation result predicts a breaking characteristic remarkably similar to experiment. The simulation results for the butterfly design are shown in figure 6.

After the simulation, elements that exceed the melting point are automatically removed. This was accomplished by using a feature of ANSYS® called element death. The contours in figure 6 show that some high temperature portions still exist in the model. These portions of the model remain because they are small portions of an element where the temperature is, on average, still cooler than the melting point of silicon. Despite this inaccuracy, the figure illustrates very similar breaking characteristics to what was observed in the experiment, as shown in figure 4(*c*).

It is important to note that while the lateral dimensions of the system are 20 μm or larger, the heat carrying the layer of the fuse-tethers is only 2 μm thick. The heat profile thus decays to a steady-state profile very quickly. There is a temperature increase on the left and right of the model, but one must remember that a constant current source is applied at these faces.

6.3. Simulation result for 'T'-design

Similar to the butterfly design, the 'T'-design follows the same patterns as the butterfly design. Figure 7 illustrates the simulation result of the 'T'-design after element death. Once again, the breaking characteristics are very similar to what was observed in the experiment, as shown in figure 5.

7. Conclusion

In this paper, a procedure to break the butterfly design and 'T'-design fuse-tethers reliably and consistently was successfully developed. Both designs yield 100% cut rates, while 15% of the cuts in the butterfly design and 20% of the cuts in the 'T'-design resulted in excessive splattering. The results from this paper conclude that the butterfly design is a better fuse-tether than the 'T'-design, due to the butterfly design's better containment of polysilicon splatter.

Due to circuit limitation and non-ideal environment, the experimental values for the Fourier number were much higher than the theoretical values. This error is largely due to the speed of the current pulse generator we used. If a faster circuit can be built, the experimental data are expected to be much closer to calculated data.

However, the ANSYS® models verified the experimental results. The breaking characteristics simulated by ANSYS® closely resembled the experimental observations. Therefore, it was confirmed that the Joule heating process can be properly simulated by the ANSYS® models.

Acknowledgments

We would like to express our gratitude to Dr Glenn Chapman and Bill Woods for their support. This project was funded by Natural Sciences and Engineering Research Council Canada, NSERC. We gratefully acknowledge the chip fabrication service of the Canadian Microelectronics Corporation (CMC).

References

[1] Pister K S J, Judy M W, Burgett S R and Fearing R S 1992 Microfabricated hinges *Sensors Actuators* A **33** 249–56
[2] Lin L Y, Lee S S, Pister K S J and Wu M C 1994 Micro-machined 3-dimensional microoptics for integrated free-space optical-system *Photon. Technol. Lett.* **6** 1445–7
[3] Johnstone R W and Parameswaran M 2004 *An Introduction to Surface-Micromachining* (Boston: Kluwer)

[4] Singh A, Horsley D A, Cohn M B, Pisano A P and Howe R T 1998 Batch transfer of microstructures using flip-chip solder bonding *J. Microelectromech. Syst.* **8** 27–33
[5] Chen J Y, Huang L-S, Chu C-H and Peizen C 2002 A new transferred ultra-thin silicon micropackaging *J. Micromech. Microeng.* **12** 406–9
[6] Faheem F F and Lee Y C 2003 Tether- and post-enabled flip-chip assembly for manufacturable rf-MEMS *Sensors Actuators* A **114** 486–95
[7] Dechev N, Cleghorn W L and Mills J K 2004 Tether and joint design for micro-components used in microassembly of 3d microstructures *Proc. SPIE* **5344** 134–46
[8] Metzger L R 1983 A 16k cmos prom with polysilicon fusible links *J. Solid-State Circuits* **18** 562–7
[9] Venkatraman P and Baliga B J 1996 Large area mos-gated power devices using fusible link technology *Trans. Electron Devices* **43** 347–51
[10] Kim O, Oh C J and Kim K S 1998 Cmos trimming circuit based on polysilicon fusing *Electron. Lett.* **34** 355–6
[11] Maier-Schneider D, Kolb S, Winkler B and Werner W M 2002 Novel surface-micromachined low-power fuses for on-chip calibration *Sensors Actuators* A **97–98** 173–8
[12] Fishbane P M, Gasiorowicz S and Thornton S T 1996 *Physics for Scientists and Engineers* 2nd edn (Upper Saddle River, NJ: Prentice-Hall)
[13] Chiu Y S and Chang K S 2005 Fuse-tethers in MEMS: theory and operation *Bachelor's Thesis* Simon Fraser University
[14] Kakac S and Yener Y 1985 *Heat Conduction* 2nd edn (Washington: Hemisphere Publishing Corporation)
[15] Koester D, Cowen A, Mahadevan R, Stonefield M and Hardy B 2003 *PolyMUMPs Design Handbook, Rev. 9.0* MEMSCAP, Bernin
[16] Shackelford J F and Alexander W 2001 *CRC Materials Science and Engineering Handbook* 3rd edn (Boca Raton: CRC Press)
[17] Johnstone R W 2005 Layout2model. http://www.sfu.ca/rjohnsto/layout2model.html [Online]
[18] Johnstone R W and Parameswaran M 2004 Modelling surface-micromachined electrothermal actuators *Can. J. Electr. Comput. Eng.* **29** 192–202
[19] Sasaki H, Ikari A, Terashima K and Kimura S 1995 Temperature dependence of the electrical resistivity of molten silicon *Japan. J. Appl. Phys.* **34** 3426–31
[20] Nagai H, Nakata Y, Tsurue T, Minagawa H, Kamada K, Gustafsson S E and Okutani T 2000 Thermal conductivity measurement of molten silicon by a hot-disk method in short-duration microgravity environments *Japan. J. Appl. Phys.* **39** 1405–8